


High-efficiency folded optics for near-eye displays

Zhenyi Luo, SID Student Member¹ | Yuqiang Ding, SID Student Member¹ |
Yi Rao² | Shin-Tson Wu, SID Fellow¹ 

¹College of Optics and Photonics,
University of Central Florida, Orlando,
Florida, USA

²Goertek Electronics, Santa Clara,
California, USA

Correspondence

Shin-Tson Wu, College of Optics and
Photonics, University of Central Florida,
Orlando, FL 32816, USA.
Email: swu@creol.ucf.edu

Funding information

GoerTek Electronics

Abstract

Pancake lens structure offers a promising solution to compact formfactor for near-eye displays. However, utilizing a half mirror to triple the optical path length causes a dramatic optical loss. The theoretical maximum optical efficiency is only 25%. To balance the tradeoff between compact formfactor and optical efficiency, here we propose a new folded optical structure with a doubled efficiency and doubled optical path length, using two polarization-selective cholesteric liquid crystal reflectors. Simulation results agree with the experiment reasonably well. Two display configurations are established to evaluate the imaging performances of the proposed pancake lens structure.

KEYWORDS

cholesteric liquid crystal, efficiency enhancement, folded optics, near-eye display

1 | INTRODUCTION

Providing new possibilities for perceiving and interacting with digital information, augmented reality (AR) and virtual reality (VR) are revolutionizing the display market. In addition to good visual experiences, such as high-resolution density, wide field of view, large eyebox, and vivid colors, wearing comfort is another critical demand for these near-eye displays. To enable long-term comfortable wearing, compact and stylish formfactor, lightweight, and low power consumption are highly desirable. To achieve these goals, tremendous efforts have been devoted to design novel optical elements and headset configurations.^{1–7}

Among these endeavors, polarization-based folded optics, also called pancake optics, has been regarded as an important step toward a compact and lightweight VR headset. The pancake system was originally proposed for flight simulators, and now, it has found renewed interest for compact VR headsets.^{8–11} Figure 1 depicts the device configuration of a conventional folded optics system. The incident circularly polarized light (solid blue line) first passes through a half mirror (HM). For convenience of discussion but without losing generality, let us assume

the outgoing light from the display panel is righthanded circularly polarized (RCP). After impinging on the HM, 50% of the RCP light is reflected by the mirror and is wasted. Upon reflection, the polarization state is converted to lefthanded circularly polarized (LCP) as indicated by the red dashed lines in the figure. For the remaining 50% of the light passing through the HM, its polarization state keeps unchanged. The output light after the quarter-wave plate (QWP) becomes linearly polarized and then is reflected by the reflective polarizer (RP). The light traveling backward to the HM turns into RCP again by the QWP. This time, only 25% of the total light is reflected by the HM (red solid line), and its polarization state is flipped to LCP to pass through the QWP and RP. Therefore, the theoretical maximum optical efficiency of such a conventional pancake lens is only 25%, but its optical path length (OPL) is tripled. Although the formfactor (depth of the headset) is reduced, the 4× lower efficiency would require a much brighter microdisplay light engine to achieve the same brightness, say 300 nits, which in turn consumes more battery power.

Cholesteric liquid crystal (CLC) elements, as a diffractive planar optics providing an ultrathin formfactor, high efficiency, and polarization selectivity, have found

promising applications for AR and VR displays.¹²⁻¹⁶ The CLC elements reflect the incident light with the same handedness as its chiral dopant and transmit the opposite component. Moreover, the reflected light can be designed to exhibit a specific phase profile, such as deflector or lens, to function as an input or output coupler for waveguide-based AR displays and Maxwellian displays.

In this paper, we demonstrate a new folded optics structure with an improved efficiency using two CLC elements as polarization-selective reflectors. In a conventional pancake optics, the OPL is tripled but its optical efficiency is reduced to 25%. Our new device configuration doubles the OPL while keeping the theoretical optical efficiency at 50%. We have fabricated the CLC elements and conducted confirming experiments to validate the designs. Simulation results also verify the improved efficiency and show the imaging performances in display systems.

2 | SYSTEM DESIGN

As described in Figure 1 for a conventional pancake optics, the combination of QWP and RP functions as a reflector for the incident RCP light, which can be replaced by a CLC element with circular polarization selectivity. Figure 2 illustrates the polarization-dependent response of a CLC element. Here, the RCP light passes through the CLC layer while the LCP light is reflected. We designate such a CLC film as CLC-L, which reflects the LCP light. Using a chiral dopant with opposite handedness, we can also fabricate a CLC-R film that reflects RCP light. To establish Bragg reflection, the required CLC layer thickness is about 10 helical pitches, which amounts to several microns.¹⁷ Depending on the phase pattern of the CLC layer, the horizontal wavevector of the reflected beam can be modulated. Therefore, CLC gratings and CLC lenses can be fabricated and are promising for advanced display systems taking the advantages of their high efficiency and compact formfactor. Another interesting feature of CLC elements is that the dispersion behavior of diffractive optics is opposite to that of refractive lens. As a result, the CLC lenses help to correct the chromatic aberration of a refractive Fresnel lens.^{18,19}

In the following, we present a new folded optics structure using the CLC elements described above. The system configuration is illustrated in Figure 3. A polarization-selective CLC reflector is applied to recycle the reflected light from HM and provide an extra OPL. The incident RCP light (blue solid line) first passes through the CLC-L, which transmits RCP light at 100%, and then impinges the HM. For the 50% transmitted light, the following path is like that of conventional structure

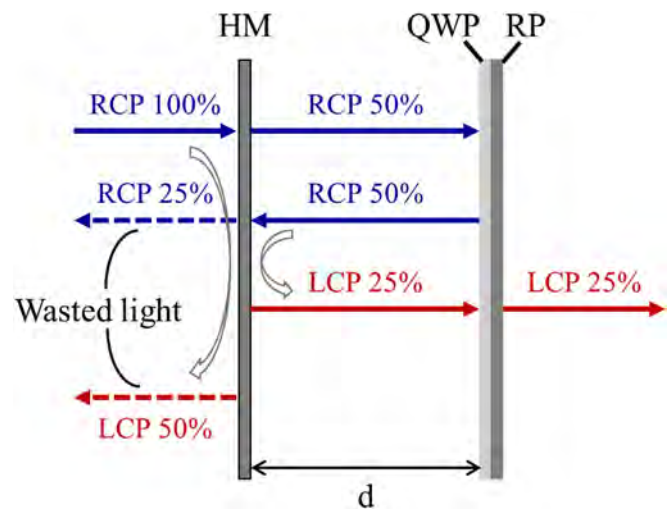


FIGURE 1 System configuration of conventional folded optics.

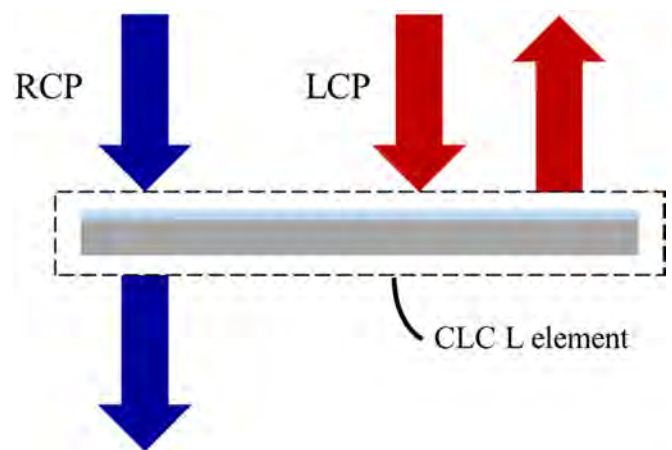


FIGURE 2 Polarization selectivity of a cholesteric liquid crystal (CLC) element.

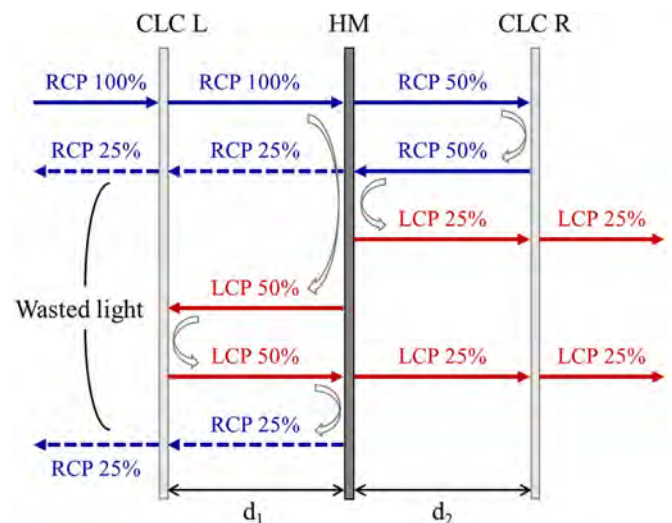


FIGURE 3 System configuration of our proposed folded optics.

described in Figure 1. Therefore, here we focus on discussing the 50% reflected light (red solid line). The HM converts the handedness of the reflected light to LCP. The light travels backward and is reflected again by the CLC-L due to its polarization selectivity. Then, the LCP light travels toward the HM again, and 25% of the light is reflected and finally wasted. Another 25% LCP light passing through the half-mirror arrives at CLC-R, which transmits RCP light at 100%. In the proposed configuration, each of the two optical paths provides 25% efficiency. To eliminate the ghost image, the OPL should be identical where the distance d_1 between CLC-L and HM equals to the distance d_2 between HM and CLC-R. In comparison, the conventional configuration provides tripled OPL with 25% efficiency and our proposed structure offers a $2\times$ OPL, but its total efficiency can be increased to 50%.

3 | DEVICE FABRICATION

The CLC element in the proposed structure only functions as a reflector for a circularly polarized light without introducing any phase profile. To correct chromatic aberrations, such a CLC element can be designed and fabricated to provide a proper optical power. The fabrication process is described in Figure 4A. To fabricate the CLC reflectors with uniform phase, the photo-alignment (PA) material Brilliant Yellow was dissolved in dimethylformamide and then spin-coated on a clean glass to form a uniform layer. Then, the PA layer was exposed using a linearly polarized collimated laser beam ($\lambda = 457$ nm) at 130 mW/cm² for 2 min. Next, the prepared CLC was spin-coated on top of the BY layer. Afterward, the CLC layer was exposed to UV light to stabilize the

polymerization process. The CLC molecules formed a helical twist as shown in Figure 4B. Two CLC elements with opposite handedness were fabricated to create a cavity in our folded optics configuration.

To prove the concept, in an experiment, we designed and fabricated the CLC elements to be effective in the blue spectral region. A broadband reflector can also be achieved using more complex fabrication process.¹⁸ Then, we measured the light leakage of the fabricated elements, and the results are shown in Figure 4C. The input light was first converted to LCP or RCP and passed through the corresponding CLC elements. Then, the transmitted light was collected by the spectrometer. These two CLC elements exhibit an efficiency of over 80% in the blue region. The leaked or transmitted light makes it easier to observe the folded images and original images in the following experiments. A nearly 100% efficiency can be obtained by increasing the CLC layer thickness.¹⁷ It is worth mentioning that the CLC layer thickness is only several micrometers, which helps to reduce the weight and formfactor of the optical system.

4 | EXPERIMENTAL RESULTS

With the fabricated CLC elements, we built the proposed folded optics system and captured images at different positions to investigate the optical efficiency enhancement. An OLED panel is used as the light engine of the system. We also measured the panel emission spectrum as shown in Figure 4C. The display panel was placed at 7 cm in front of the first CLC element, and the emitted light was converted to RCP using a circular polarizer. The cavity length (d_1 and d_2) is 6 cm. Here, we intentionally enlarged the system size for easier evaluation of

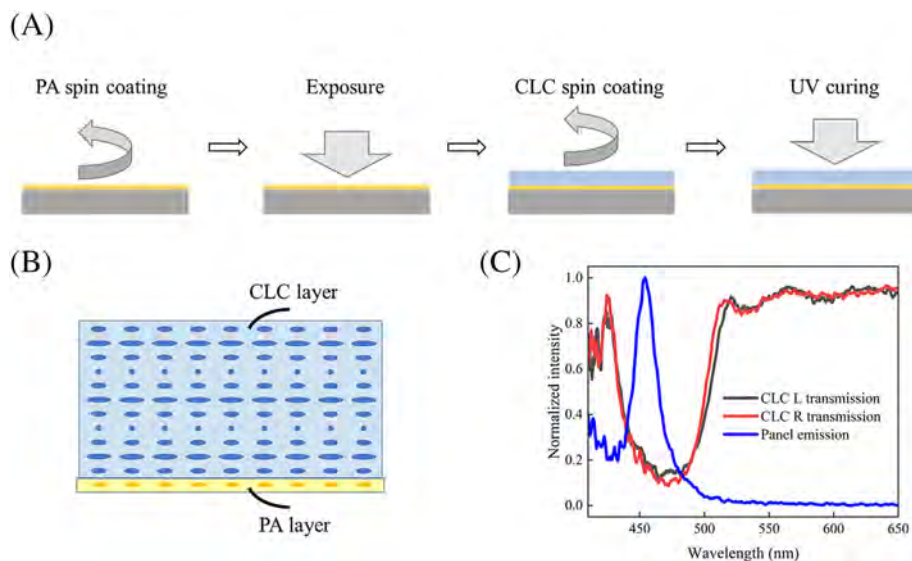


FIGURE 4 (A) Fabrication of cholesteric liquid crystal (CLC) elements, (B) Helical twist structure of the CLC layer, and (C) measured transmittance of the CLC elements and emission spectrum of display panel.

the proposed system. Figure 5 depicts the captured images.

Figure 5A is the original image from the display panel. The folded image is shown in Figure 5B, where two images can be observed simultaneously. The clear one is the desired folded image, and the blurred one is the leakage of the original image, which can be differentiated by their sizes. The size of folded image is smaller than that of the original one because the OPL is folded, which gains an extra 12 cm in length. We also focus on the leaked image shown in Figure 5C, which indicates a different OPL. Moreover, to compare the efficiency of our new configuration with conventional structure, we removed the first CLC element and the remaining system shared the same principle with conventional folded systems. Figure 5D shows the result of this CLC-based pancake image. The image in Figure 5B is much brighter than that in Figure 5D, indicating a noticeable efficiency improvement of our new folded optics system. Table 1 summarizes the object distance and normalized irradiance of three different layouts for better understanding.

To analyze the enhancement quantitatively, the images were first converted to grayscale images. To eliminate the leakage in Figure 5, we set a threshold to extract the desired images. Results are shown in Figure 6. The enhanced brightness can be clearly observed using naked eyes by comparing Figures 6(B) and 6(C). More specifically, the total efficiency of CLC pancake system is 20.5%, and our proposed system is 32.2%, indicating a $1.57\times$ higher brightness. The brightness is not doubled as we initially expected because the efficiency of CLC elements

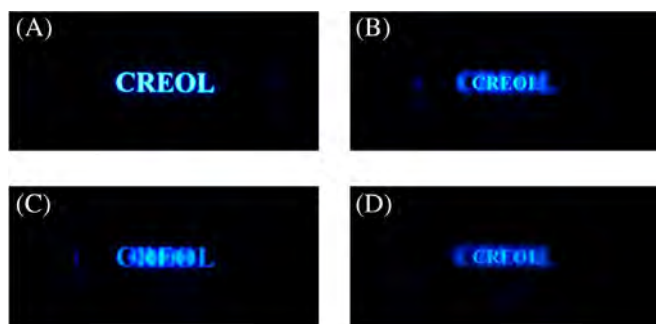


FIGURE 5 (A) Original image, (B) folded image, (C) leaked image, and (D) cholesteric liquid crystal (CLC)-based pancake image.

TABLE 1 Summary of three different layouts.

Summary	Figure 5A	Figure 5B	Figure 5C
Object distance (cm)	25.5	37.5	37.5
Normalized irradiance	100%	32.2%	20.5%

does not reach 100% in our experiment, which can be optimized by increasing the CLC layer thickness.

5 | SIMULATION RESULTS

To further investigate the performances of our proposed system, we designed a simulation tool using Zemax. The CLC reflectors model was built based on rigorous coupled-wave analysis (RCWA) method.²⁰ First, we studied the influence of CLC efficiency over leakage. The system configuration is like our experiment. The display panel is placed close to the first CLC reflector to maximize the folded OPL. The HM is at the middle of the two reflectors in order to eliminate the ghost image. After passing through the system, the light will be collected by the detector.

Ghost image of leakage is observed in our experiments due to the 80% efficiency. The efficiency of a CLC reflector is determined by its layer thickness; a higher optical efficiency can be achieved by increasing the pitch number but will gradually saturate when the pitch number exceeds 10.¹⁷ As observed in Figure 7, the ghost image became invisible, and the effective irradiance of the desired image also increases using a CLC reflector with a higher efficiency.

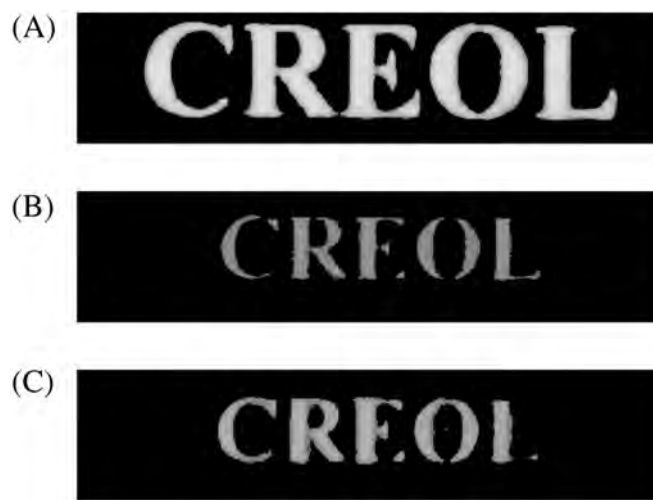


FIGURE 6 Grayscale images of (A) original image, (B) cholesteric liquid crystal (CLC)-based pancake image, and (C) folded image.

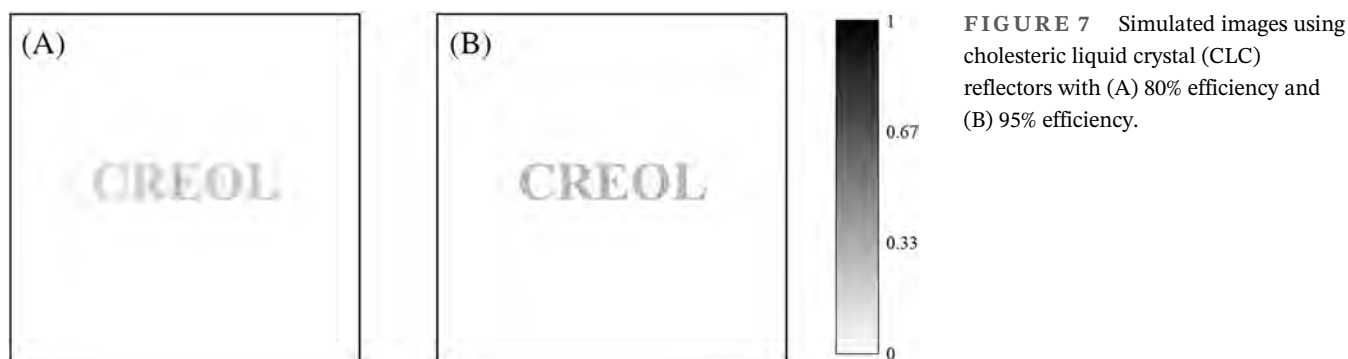


FIGURE 7 Simulated images using cholesteric liquid crystal (CLC) reflectors with (A) 80% efficiency and (B) 95% efficiency.

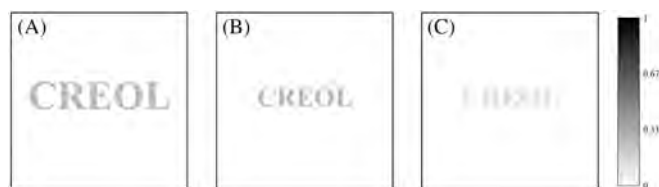


FIGURE 8 Simulated results of (A) original image, (B) folded image, and (C) cholesteric liquid crystal (CLC)-based pancake image.

The efficiency of the proposed system is also studied in this simulated model. The original image is captured by the detector as shown in Figure 8A. Then, we simulated the folded image using CLC reflectors with an efficiency of over 95%, and the result is shown in Figure 8B. The size of the image becomes smaller as the object distance gets larger. The total power received by the detector is also decreased, leading to an efficiency of 49.96% as we expected. The image of CLC-based pancake system is also simulated as shown in Figure 8C for comparison. These two images show the same size because the folded optical paths are the same, which is similar to the experimental results. As discussed before, a conventional pancake system provides $3\times$ OPL, and our new system offers only $2\times$ OPL. However, considering the case when the object position is not close to the HM in the conventional system, the two systems provide the same extra OPL. The efficiency of the CLC-based pancake system is only 24.92%. Therefore, the efficiency of folded optics is doubled with our proposed configuration.

In addition to doubled efficiency of the new system, we also evaluate the imaging performance in a VR system as illustrated in Figure 9A. A collimation lens with a focal length of 40 mm is placed right after the second CLC reflector and the display panel is close to the first one. The distance between display panel and collimation lens is 20 mm, which will be doubled by the folded structure to fit the focal length. The collimated beam after the lens

is received by the eye. Figure 9B is the original object, and the captured image is shown in Figure 9C.

Next, we simulate the structure that the lens is sandwiched between the CLC reflectors and the HM. In this optical layout, instead of considering the OPL, providing the same optical power for the two paths is essential to eliminate the ghost images. Due to the symmetry of the two optical paths, mirrored imaging optics should be placed on both sides of the HM to offer the same magnification and depth as shown in Figure 10A. For each path, the light will travel through the lenses four times. The focal length of the two lenses is 100 mm. Therefore, the theoretical effective focal length of the combined system should be around 25 mm considering the compact configuration. In the simulated system, the distance between the display panel and the HM is 24.8 mm, which agrees with our expectation. The captured image is shown in Figure 10B.

The above two systems show decent imaging performances. By comparing the captured images in the two systems, we found that the configuration in Figure 10 provides a higher efficiency. The reason for the difference comes from the longer OPL in Figure 9. Therefore, the emitted Lambertian light may escape from the system while traveling inside the cavity. Instead of folding a longer OPL, the system in Figure 10 provides a higher optical power for achieving a more compact formfactor. However, the accumulated aberrations after passing through the lenses four times in the system may lead to chromatic aberrations. This would affect the final image performances. Fortunately, the chromatic aberration of a diffractive CLC reflector can be corrected by a properly designed refractive lens, which has been proven in conventional pancake systems.^{18,19}

As discussed before, we use a CLC reflector to replace the QWP and RP in conventional pancake system. It not only offers an ultrathin formfactor, which is usually several micrometers, but also brings advantages including chromatic aberrations correction and avoiding clocking

FIGURE 9 (A) System configuration, (B) original image, and (C) captured image.

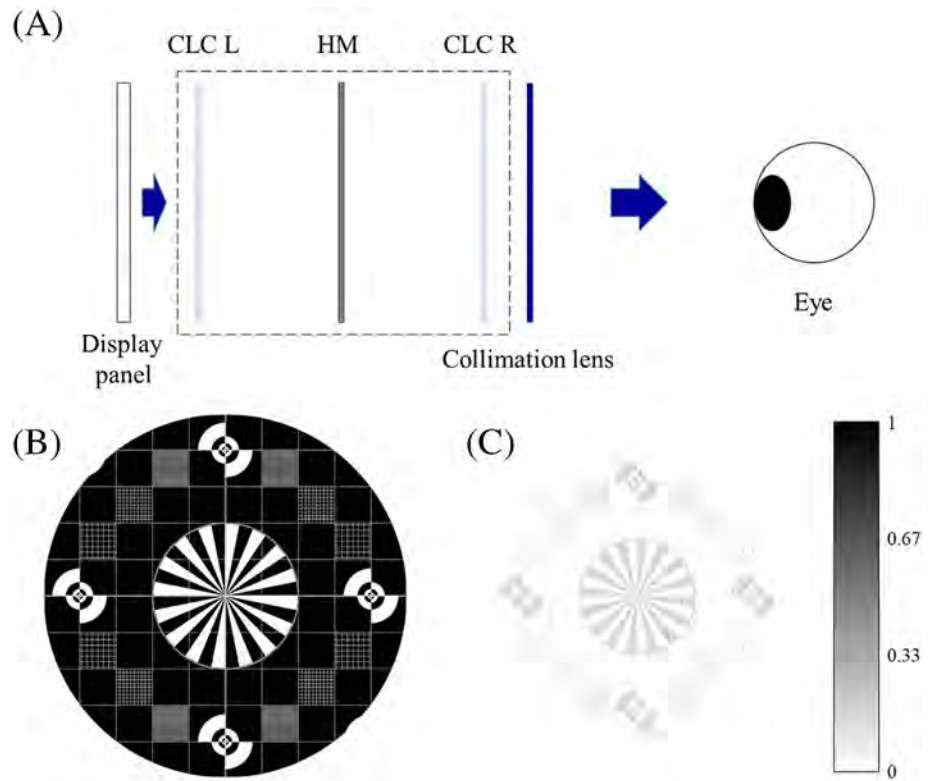
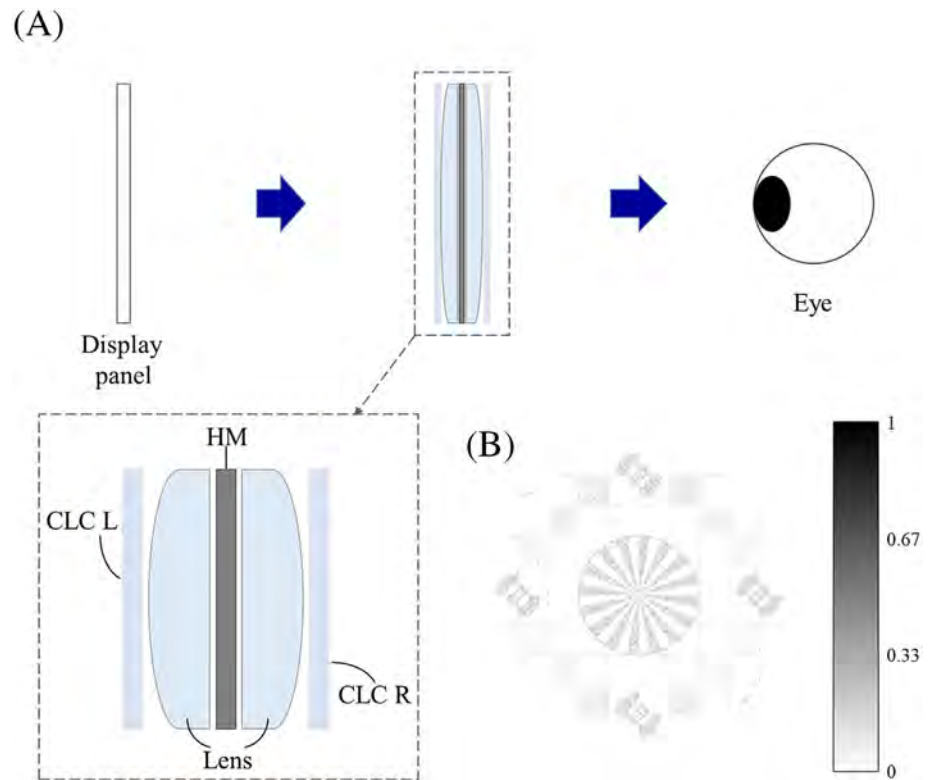


FIGURE 10 (A) System configuration, (B) captured image.



angle alignment between the QWP and the RP. In a conventional pancake system, to convert the incident circularly polarized light to linearly polarized with a desired angle, the optical axis of the QWP should be aligned carefully, or a ghost image can be generated, which would be

no longer a problem after the adoption of CLC reflectors. Moreover, our CLC reflectors can be made to have a lens phase profile to offer a proper optical power to improve the color performance of the system. Simulations have been conducted to prove the concept of correcting

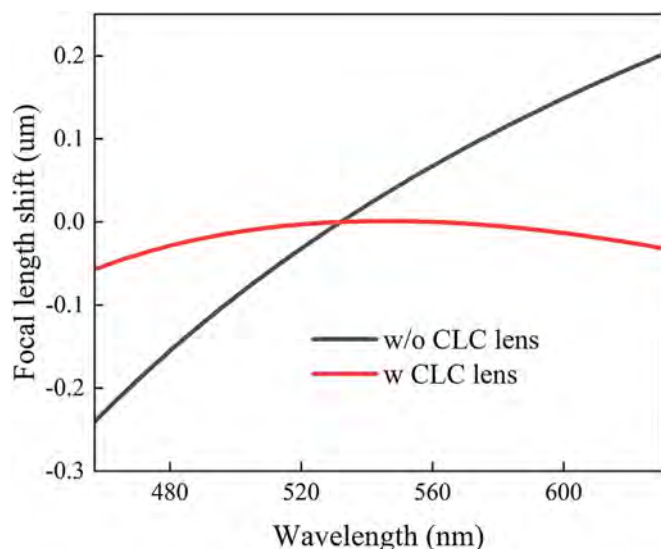


FIGURE 11 Focal length shift of the system with and without cholesteric liquid crystal (CLC) lens.

chromatic aberrations, and the results are illustrated in Figure 11. Here, black line represents the focal length shift without the CLC lens. Then, we apply a CLC lens with a 50-cm focal length at 457 nm, and the results are shown in red line. Improved color performances can be easily observed after using the CLC lens.

6 | CONCLUSION

We proposed an efficiency-enhanced folded optics system with two CLC reflectors. Each reflector functions as a combined QWP and RP to reflect a specific circularly polarized light. Besides, the CLC reflectors designed to have a lens phase profile help correct the chromatic aberrations for the imaging optics. In the proposed system, the reflected light that is wasted in conventional folded optics is partially recycled using our CLC reflectors. Both experimental and simulated results confirm the efficiency enhancement of our proposed system. Theoretically, the efficiency should be doubled in comparison with conventional pancake structure. However, our experiment only shows $1.57\times$ enhancement because our CLC reflectors are not ideal. Though the OPL is tripled in conventional pancake system, we notice that our new folded optics system also enables same OPL when the display panel is not close to the HM in the pancake system. Moreover, we built two display systems to further investigate the imaging performances of the new folded optics configuration. With doubled optical efficiency, our new system is promising for near-eye display systems with a lower power consumption and compact formfactor.

ACKNOWLEDGMENTS

The UCF group is indebted to GoerTek Electronics for the financial support and Qian Yang and Yannanqi Li for their stimulating discussions.

ORCID

Shin-Tson Wu  <https://orcid.org/0000-0002-0943-0440>

REFERENCES

- Chang C, Bang K, Wetzstein G, Lee B, Gao L. Toward the next-generation VR/AR optics: a review of holographic near-eye displays from a human-centric perspective. *Optica*. 2020;7(11):1563–1578. <https://doi.org/10.1364/OPTICA.406004>
- Maimone A, Wang J. Holographic optics for thin and lightweight virtual reality. *ACM Trans Graph (TOG)*. 2020;39(4):67. <https://doi.org/10.1145/3386569.3392416>
- Xiong J, Hsiang EL, He Z, Zhan T, Wu ST. Augmented reality and virtual reality displays: emerging technologies and future perspectives. *Light Sci Appl*. 2021;10(1):216. <https://doi.org/10.1038/s41377-021-00658-8>
- Cakmakci O, Qin Y, Bosel P, Wetzstein G. Holographic pancake optics for thin and lightweight optical see-through augmented reality. *Opt Express*. 2021;29(22):35206–35215. <https://doi.org/10.1364/OE.439585>
- Lu Y, Li Y. Planar liquid crystal polarization optics for near-eye displays. *Light Sci Appl*. 2021;10(1):122. <https://doi.org/10.1038/s41377-021-00567-w>
- Ratcliff J, Supikov A, Alfaro S, Azuma R. ThinVR: heterogeneous microlens arrays for compact, 180 degree FOV VR near-eye displays. *IEEE Trans vis Comput Graph*. 2020;26(5):1981–1990. <https://doi.org/10.1109/TVCG.2020.2973064>
- Park HS, Hoskinson R, Abdollahi H, Stoeber B. Compact near-eye display system using a superlens-based microlens array magnifier. *Opt Express*. 2015;23(24):30618–30633. <https://doi.org/10.1364/OE.23.030618>
- LaRussa JA, Gill AT. The holographic pancake window TM. In: *Visual Simulation and Image Realism I* 162 SPIE; 1978. p. 120–129.
- Wong TL, Yun Z, Ambur G, Etter J. Folded optics with birefringent reflective polarizers. In: *Digital Optical Technologies SPIE* 10335; 2017. p. 84–90.
- Lee S, Wang M, Li G, Lu L, Sulai Y, Jang C, et al. Foveated near-eye display for mixed reality using liquid crystal photonics. *Sci Rep*. 2020;10(1):16127. <https://doi.org/10.1038/s41598-020-72555-w>
- Geng Y, Gollier J, Wheelwright B, Peng F, Sulai Y, Lewis B, et al. Viewing optics for immersive near-eye displays: pupil swim/size and weight/stray light. In: *Digital Optics for Immersive Displays SPIE*; 2018;10676:19–35.
- Kobashi J, Yoshida H, Ozaki M. Planar optics with patterned chiral liquid crystals. *Nat Photonics*. 2016;10(6):389–392. <https://doi.org/10.1038/nphoton.2016.66>
- Xiong J, Wu ST. Planar liquid crystal polarization optics for augmented reality and virtual reality: from fundamentals to applications. *eLight*. 2021;1(1):3. <https://doi.org/10.1186/s43593-021-00003-x>
- Chen Q, Peng Z, Li Y, Liu S, Zhou P, Gu J, et al. Multi-plane augmented reality display based on cholesteric liquid crystal

- reflective films. *Opt Express*. 2019;27(9):12039–12047. <https://doi.org/10.1364/OE.27.012039>
15. Yin K, Zhan T, Xiong J, He Z, Wu ST. Polarization volume gratings for near-eye displays and novel photonic devices. *Crystals*. 2020;10(7):561. <https://doi.org/10.3390/cryst10070561>
 16. Yin K, Hsiang EL, Zou J, Li Y, Yang Z, Yang Q, et al. Advanced liquid crystal devices for augmented reality and virtual reality displays: principles and applications. *Light Sci Appl*. 2022; 11(1):161. <https://doi.org/10.1038/s41377-022-00851-3>
 17. Lee YH, Yin K, Wu ST. Reflective polarization volume gratings for high efficiency waveguide-coupling augmented reality displays. *Opt Express*. 2017;25(22):27008–27014. <https://doi.org/10.1364/OE.25.027008>
 18. Li Y, Zhan T, Yang Z, Xu C, LiKamWa PL, Li K, et al. Broadband cholesteric liquid crystal lens for chromatic aberration correction in catadioptric virtual reality optics. *Opt Express*. 2021;29(4):6011–6020. <https://doi.org/10.1364/OE.419595>
 19. Zhan T, Zou J, Xiong J, Liu X, Chen H, Yang J, et al. Practical chromatic aberration correction in virtual reality displays enabled by large-size ultra-broadband liquid crystal polymer lenses. *Adv Opt Mater*. 2020;8(2):1901360. <https://doi.org/10.1002/adom.201901360>
 20. Xiong J, Wu ST. Rigorous coupled-wave analysis of liquid crystal polarization gratings. *Opt Express*. 2020;28(24):35960–35971. <https://doi.org/10.1364/OE.410271>

How to cite this article: Luo Z, Ding Y, Rao Y, Wu S-T. High-efficiency folded optics for near-eye displays. *J Soc Inf Display*. 2023;31(5):336–43. <https://doi.org/10.1002/jsid.1207>

AUTHOR BIOGRAPHIES



Zhenyi Luo received his BE degree from the Department of Precision Instrument at Tsinghua University, China, and MS degree from the Department of Chemistry at the University of Tokyo, Japan. Now, he is a PhD student at the College of Optics and Photonics, University of Central Florida. His research interests include advanced augmented reality

and virtual reality displays, and novel liquid crystal devices.

Yuqiang Ding received his BS degree in Optical Engineering from Shandong University, China, in 2021. He is currently working toward a PhD at the College of Optics and Photonics, University of Central Florida. His current research interests include novel liquid crystal optical elements and optical system design in near-eye displays.

Yi Rao received his BS and MS degrees from Tsinghua University, China. He received his PhD degree in Electrical Engineering and Computer Science from the University of California, Berkeley, in 2012. He founded Bandwidth10 in 2011 and became Director of augmented reality at Rokid from 2015 to 2019. Presently, he is the general manager of Goertek Electronics.

Shin-Tson Wu is a Trustee Chair professor at the College of Optics and Photonics, University of Central Florida (UCF). He is an Academician of Academia Sinica, a Charter Fellow of the National Academy of Inventors, and a Fellow of the IEEE, OSA, SID, and SPIE. He is a recipient of the Optica Edwin H. Land Medal (2022), SPIE Maria Goeppert-Mayer Award (2022), Optica Esther Hoffman Beller Medal (2014), SID Slottow-Owaki Prize (2011), Optica Joseph Fraunhofer Award (2010), SPIE G. G. Stokes Award (2008), and SID Jan Rajchman Prize (2008). In the past, he served as the founding Editor-In-Chief of the *Journal of Display Technology*, Optica publications council chair and board member, and SID honors and awards committee chair.